JOURNAL OF Applied Polymer SCIENCE

Study of Poly(vinyl chloride)/Acrylonitrile-Styrene-Acrylate Blends for Compatibility, Toughness, Thermal Stability and UV Irradiation Resistance

Yunxiang Zhang, Yingjie Xu, Yihu Song, Qiang Zheng
MOE Key Laboratory of Macromolecular Synthesis and Functionalization, Department of Polymer Science and Engineering, Zhejiang University, Hangzhou 310027, China
Correspondence to: Y. Song (E-mail: s_yh0411@zju.edu.cn)

ABSTRACT: A novel rigid poly(vinyl chloride) (PVC)/acrylonitrile–styrene–acrylate (ASA) copolymer blend with good ultraviolet (UV) irradiation resistance and toughness was reported. ASA with good weatherability and toughness was mixed with PVC by conical twin-screw extruder to improve the UV irradiation resistance and toughness of PVC. The blends were characterized using Fourier-transform infrared spectra, dynamic mechanical analysis, and scanning electron microscope. Notch Charpy impact test was used to characterize the UV radiation induced changes in toughness. The results showed that ASA was able to toughen PVC with simultaneously improving heat resistance, thermal stabilization, and protecting PVC from irradiation photochemical degradation. © 2013 Wiley Periodicals, Inc. J. Appl. Polym. Sci. 130: 2143–2151, 2013

KEYWORDS: poly(vinyl chloride); thermal properties; compatibilization; blends

Received 23 October 2012; accepted 9 April 2013; Published online 16 May 2013
DOI: 10.1002/app.39405

INTRODUCTION

Rigid PVC is used in a wide range of applications including pipes, gutters, and window profiles. However, the two defects, low heat distortion temperature (HDT), and low notch impact strength, limit its application.[1] HDT might be largely improved with a wide range of additives. High softening point poly(α-methylstyrene-*co*-acrylonitrile) can improve HDT but embrittle PVC.[2] Nitrile rubber,[3] acrylonitrile–butadiene–styrene (ABS),[4–6] methylmethacrylate–butadiene–styrene (MBS), and methyl methacrylate–acrylonitrile–butadiene–styrene (MABS) resins[7] have been extensively used to toughen PVC due to good interfacial adhesive interaction between the PVC matrix and the well-dispersed rubber particles, however, which usually lead to degraded tensile strength and modulus.[8] Core–shell structured MBS resin is one of the most effective impact modifiers commonly used in transparent PVC products with improved toughness.[9]

PVC products are readily attacked by UV light, resulting in discoloration and losses of properties in particular gloss, strength, and toughness. High heat-resistant ABS could improve HDT without sacrificing impact strength, while the unsaturated polybutadiene rubber is unstable to heat and UV light, gradually losing its elastomeric performance and tending to yellow over time. Toughening PVC using ABS, MBS, and MABS in general introduces additional photo-oxidation of polybutadiene, which accelerates the discoloration. Prior thermal treatment of both PVC and impact modified PVC even accelerates the photo-oxidative degradation.[7]

ASA resins are prepared by grafting copolymerization of styrene and acrylonitrile monomers onto acrylate rubber particles. Rather than the UV sensitive polybutadiene rubber in ABS, ASA contains acrylate rubber to provide high impact strength and exceptional resistance to degradation and yellowing under UV radiation and atmospheric oxygen. ASA with typical HDT (~90°C at 1.8 MPa) is higher than PVC (~70°C) possesses of superior weatherability, impact, and chemical resistances[10,11] and has been blended with many polymers to make alloys with outstanding impact resistance and excellent weatherability. ASA is recently used to toughen bisphenol A polycarbonate[10] and a small amount styrene–acrylonitrile (SAN) resin could improve the rubber dispersion contributing to high impact strength of blends.[11] ASA is expected to improve HDT of PVC without sacrificing toughness. PVC/ASA (50/50 by weight) blend has been used to prepare high impact strength coconut fiber composite.[12]

A common industrial technology is using ASA as a cap layer to protect PVC products from discoloration.[13] PVC products covered with ASA are usually prepared via multilayer coextrusion, however, structure and properties of PVC/ASA blends prepared

Table I. Formulation of PVC/ASA Blends

Sample ingredients (phr)[a]	1#	2#	3#	4#	5#	6#
PVC	100	100	100	100	100	100
ASA	0	20	40	60	80	100
Dibutyltin dilaurate	3	3	3	3	3	3
Glyceryl monosterate	2	2	2	2	2	2
Acrylic processing aid	3	3	3	3	3	3
Oxidized polyethylene wax	1	1	1	1	1	1

[a] phr: parts per hundred of resin.

by molding injection are rarely investigated. In this article, ASA is used to toughen the rigid PVC and improve heat and UV irradiation resistances. Influences of ASA content on structures and properties of the blends are discussed.

EXPERIMENTAL

Materials

PVC (S-1000, weight-averaged molecular weight 98,000, Qilu Petrochem. Co., Shandong, China), ASA (Li-912, LG Chem., Korea), dibutyltin dilaurate (HTM-2010, Haipudun Chem. Co., Zhejiang, China), glyceryl monosterate (GMS, Hangzhou Oil and Fat Chem. Co., Zhejiang, China), acrylic processing aid (ACR, 401, Hangzhou Chuanhua Co., Zhejiang, China), oxidized polyethylene wax (OPE, Shanghai Huayi Plastics Co., Shanghai, China) were used as received for preparing PVC/ASA blends.

Sample Preparation

PVC and other components were mixed in a high-speed mixer following the formulation in Table I, which mixed by a high-speed mixer (Wuhan Yiyang Plastics Machinery Co., Hubei, China). The mixtures were melt blended in a conical twin-screw extruder (Wuhan Yiyang Plastics Machinery Co., Hubei, China) with temperatures maintained at 167, 172, 173, and 170°C from the hopper to the die. The extrudate was pelletized by hot cutting and injection molded into notched impact specimens by an injection molding machine (Boy 55, Boy, Germany).

Characterization

Congo red test was performed for evaluating thermal stability of the blends according to ASTM D4202. The PVC mixtures in powder form were put into a tube with Congo red test paper located 2.5 cm above the sample. The tube was heated in a glycerol bath at 180°C to evaluate static thermal stability time (t_{ss}) defined as the time when the Congo red test paper began to turn blue.

Vicat softening test was carried out on a Vicat softening tester (CEAST Sci. Instruments Co., Italy) at a weight of 10 N with a heating rate of 50°C/h. Vicat softening temperature (T_v) was recorded when the needle penetrated 1 mm from the surface into the samples.

Accelerated artificial UV-weathering test was conducted with an ultraviolet light aging test chamber (Q8/UV2, Dongguan Horngjaan Equipment Co., Guangdong, China). The gap between the lamp surface and the samples was 50 mm. The samples were subjected to continuous exposures of averaged intensity 0.68 W/m^2 with the wavelength of 315–400 nm to predetermined times at 60 ± 1°C.

Fourier-transform infrared (FTIR) spectra were recorded on a FTIR spectrometer (Perkin-Elmer System 2000, Perkin-Elmer Co.) at a nominal resolution of 2 cm^{-1}. The samples in powder form were mixed with potassium bromide and compressed into transparent discs for FTIR test.

The dispersion of ASA in the blend was examined using transmission electron microscopy (TEM, JEM-1230, JEOL, Japan) with an accelerating voltage of 90 kV. Ultrathin sections of 150–200 nm were cut from the cross section of injection-molded bars by a microtome (LKB-5, LKB Co., Switzerland). Osmium tetroxide (OsO_4) was used to stain the samples.

Scanning electron microscope (SEM, S-4800, Hitachi Co., Japan) was used to examine the morphology of blends. The fracture surfaces of the specimens were used for morphology observation after being coated with gold.

Dynamic mechanical analysis (DMA) was performed on a dynamic mechanical thermal analyzer (DMA 242, NETZSCH, Germany) with a single cantilever geometry. Specimens with a size of 4 × 10 × 40 mm^3 were submitted to sinusoidal deformation of 0.2 μm amplitude at frequency 1 Hz from −120°C to 180°C at a heating rate of 3°C/min.

Notched Charpy impact tests were carried out by a pendulum impact testing machine (ZBC 1400-2, MTS Systems Co., China). The specimens were equilibrated in a thermostatic container (MT3065, Guangzhou ESPEC Environmental Equipment Co., China) for more than 2 h at prescribed temperatures, and taken out quickly for impact tests. Impact strength was evaluated from at least 10 specimens for each set of samples.

RESULTS AND DISCUSSION

Figure 1(a) shows FTIR spectra of PVC, ASA, and PVC/ASA (100/60 by weight) blend. PVC exhibits characteristic peaks at 619 and 700 cm^{-1} assigned to C–Cl stretching vibration and a peak at 1429 cm^{-1} to CH_2 deformation vibration. The absorbances at 1672 and 1732 cm^{-1} in PVC spectra are assigned to C=O vibrations in ACR and dibutyltin dilaurate.[14] ASA exhibits a broad C=O stretching peak at 1735 cm^{-1}, a tiny nitrile peak at 2236 cm^{-1}, benzene ring stretching vibrations at 1452, 1495, and 1603 cm^{-1} and flexural vibrations at 701 and 762 cm^{-1}.[15] The C=O band in the 1760–1710 cm^{-1} range can be decomposed into two single peaks centered at 1735 and 1722 cm^{-1} assigned to the free and the hydrogen bonded C=O groups, respectively,[16] as shown as dotted curves in Figure 1(b). Percentages of the hydrogen bonded C=O group are estimated at 9.7, 14.4, and 29.0%, respectively, for PVC, the blend and ASA according to $A_{1722}/(A_{1735} + A_{1722})$. Here, A_{1735} and A_{1722} are area absorbances of the single components at 1735 and 1722 cm^{-1}, respectively. In the PVC/ASA blend, the nitrile peak at 2236 cm^{-1} in pure ASA shifts to 2239 cm^{-1} and the C–Cl stretching peak at 834 cm^{-1} in pure PVC shifts to 842 cm^{-1}, indicating the existence of electron transfer interactions between ASA and PVC.[17,18] These are formed partially at the expense of

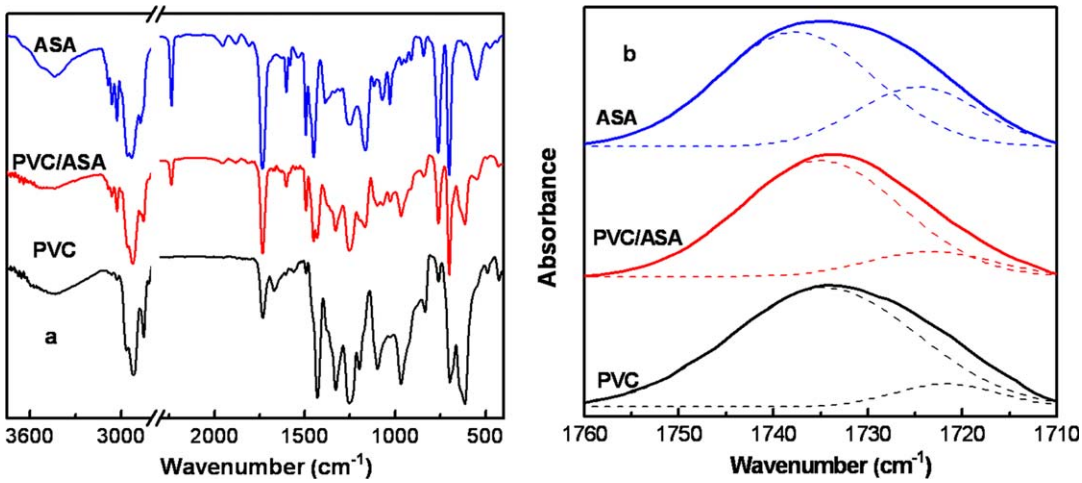

Figure 1. FTIR spectra of PVC, ASA, and PVC/ASA (100/60 by weight) blend. [Color figure can be viewed in the online issue, which is available at wileyonlinelibrary.com.].

the disruption of electron transfer complexes between butyl acrylate and acrylonitrile co-monomers within ASA, since the C≡N stretching vibration shifts to slightly higher wavenumbers.[19] This interaction is helpful for the miscibility of the blend.[17–19]

Figure 2 shows storage modulus (E') and loss factor (tan δ) against temperature (T) for PVC, ASA, and PVC/ASA blends at 1 Hz. PVC experiences a weak β-transition from -100°C to 20°C ascribed to the localized conformational motions,[20] as distinguished from the broad tan δ peak and the slight E' depression. E' at α-(glass) transition drops sharply by two orders of magnitude. The β-and the α-transition temperatures (T_β and T_g) of PVC are determined at -50.0°C and 92.0°C, respectively, according to the peak temperatures of the tan δ curves. ASA exhibits a weak and a strong transition at -33.7 and 124.2°C referring to T_g of the soft acrylate rubber phase and T_g of the rigid SAN phase, respectively. T_β of PVC is close to T_g of the acrylate rubber phase in ASA. The tan δ curves of PVC/ASA

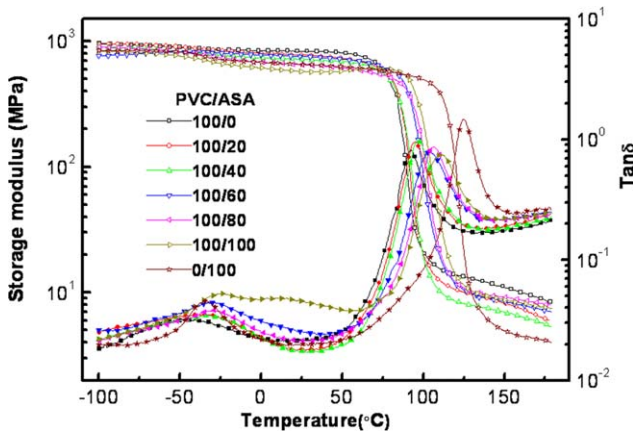

Figure 2. Storage modulus (E', hollow symbols) and loss factor (tan δ, solid symbols) against temperature (T) for PVC, ASA, and PVC/ASA (w/w) blends. [Color figure can be viewed in the online issue, which is available at wileyonlinelibrary.com.]

blends exhibit two regions of thermal transitions. The α-transitions of PVC and the rigid SAN phase in ASA merge into a single T_g peak located between those of PVC and ASA, indicating a good compatibility between the PVC matrix and the SAN phase of ASA. This peak shits to higher temperatures with increasing ASA content. The strong PVC/SAN interfacial interaction hinders PVC chains to move, further suppresses the glass transition of the acrylate rubber phase covalently bonded to the SAN phase, giving rise to an increase in T_g of the acrylate rubber phase in the blend. When ASA content reaches 100 phr in the blend, a secondary relaxation peak appears in 15.8°C, which is a result of intermolecular interactions between PVC and ASA. These results account for the good compatibility between PVC and the SAN phase in ASA.[21]

Figure 3 shows TEM images of PVC/ASA blends at two different compositions. The blends contain well dispersed domains in white color of typical 100–300 nm in diameter, which is assigned to the acrylate rubber phase in ASA. The rigid SAN phase in ASA is well mixed with the PVC matrix to form a continuous phase, which is attributed to the interaction between PVC and SAN.[21]

PVC presents an obvious drawback due to its low thermal stability despite being one of the most demanded versatile thermoplastics worldwide. Stabilizers such as lead salts,[22] organotins,[23] soaps,[24] and rare earth compounds[25] must be incorporated in order to restrain PVC degradation during thermal processing, mainly through absorption of hydrochloric acid released from PVC partial decomposition or substitution of labile sites of partially decomposed PVC macromolecules.[26] Organo-tin stabilizer of 3 phr is used here for stabilizing PVC and its blends. Figure 4 shows influence of ASA content on t_{ss} measured at 180°C. t_{ss} of PVC is about 5 min while it increases significantly with increasing ASA content and reaches 25 min at 100 phr ASA. It is clear that ASA could improve thermal stabilization of PVC markedly, which is quiet favorable for preparing rigid PVC products by injection molding. The highly polar PVC molecules may share electrons to some extent with ASA,[27] which pulls on and

Applied Polymer SCIENCE

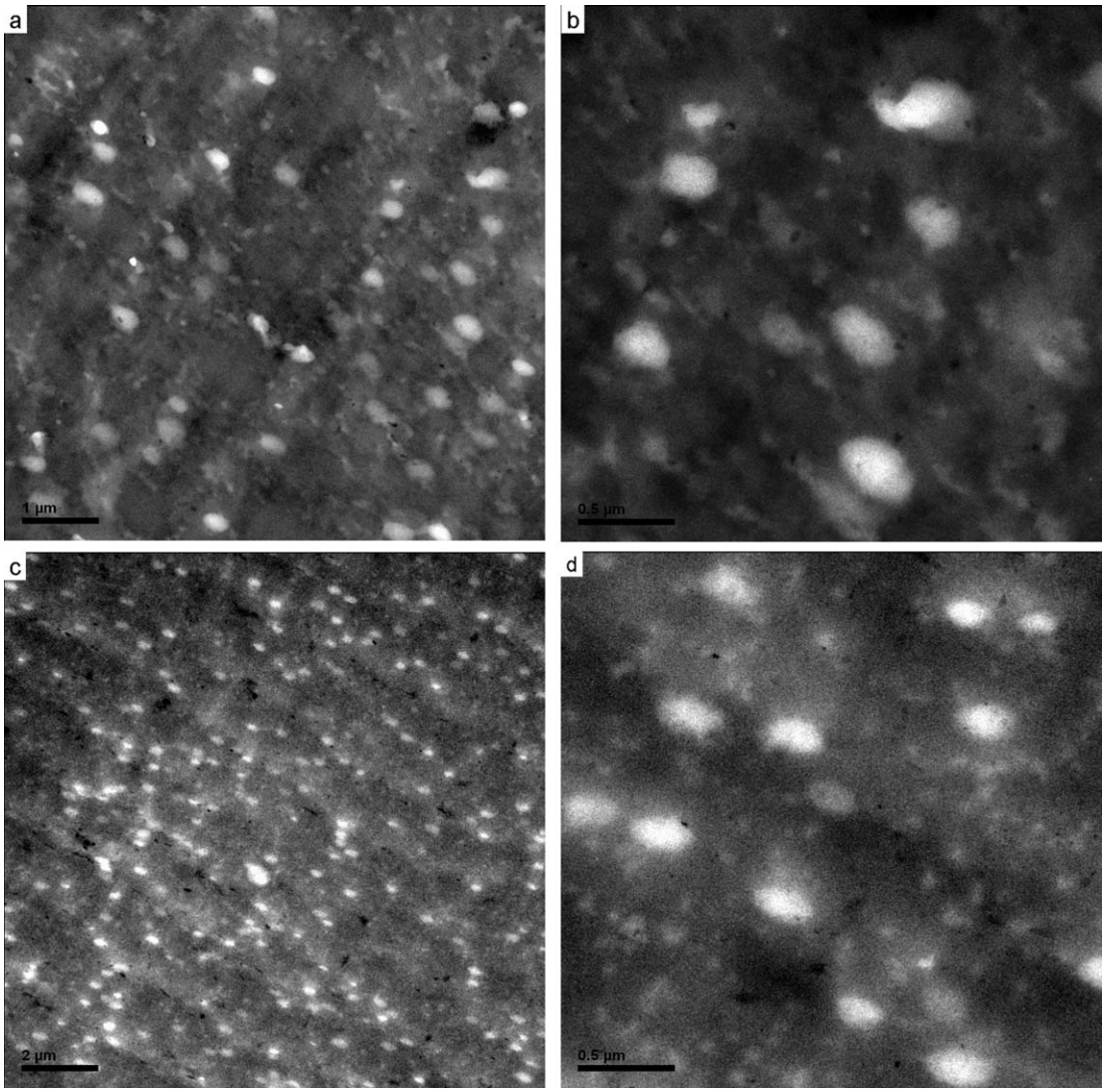

Figure 3. TEM micrographs of PVC/ASA blends containing (a,b) 60 phr and (c,d) 100 phr ASA.

weakens the C–H and C–Cl bonds, and improves the thermal stability of PVC. The interaction between chlorines of PVC and the ester carbonyl groups in polyesters can delay the detachment of the labile chlorine atoms.[28]

Vicat softening temperature (T_v) was used to evaluate heat resistance of the blends. Also shown in Figure 4 is T_v as a function of ASA content. Unlike other modifier used to toughen PVC usually leading to a reduction in T_v,[29] T_v of injection molded rigid PVC is 78.6°C while it shows tremendous improvement with increasing ASA content, to 90.8°C for the blend with 100 phr ASA. The intermolecular interaction between ASA and PVC may play a key role in heat resistance of the blends[30] and the T_v raise may be also related to the raise of T_g.[31]

Figure 5(a) shows influence of ASA content on notched Charpy impact strength of the blends at three different temperatures. A sharp brittle–ductile transition (BDT) occurs at critical ASA contents depending on T. The impact strength beyond BDT may be higher than those of pure PVC and ASA, suggesting a

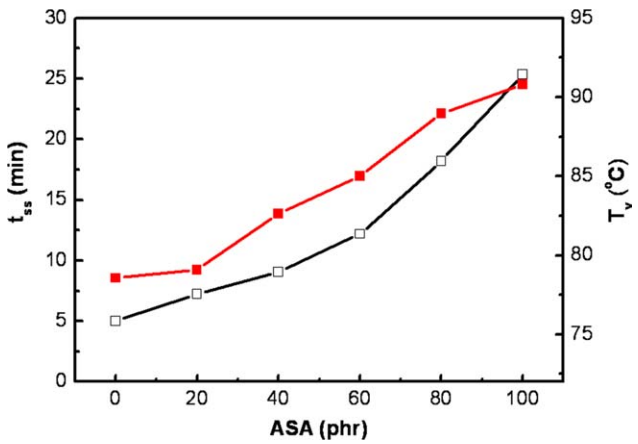

Figure 4. Influence of ASA content on static stability time (t_{ss}, hollow symbols) at 180°C and Vicat softening temperature (T_v, solid symbols) for the blends. [Color figure can be viewed in the online issue, which is available at wileyonlinelibrary.com.]

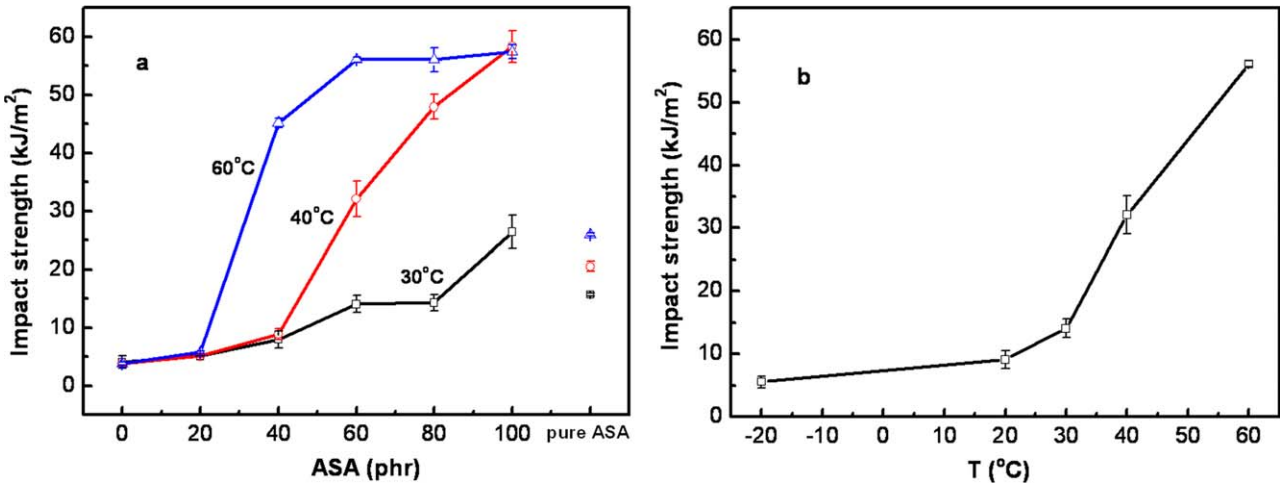

Figure 5. Plots of notched Charpy impact strength (a) against ASA content for blends at three different temperatures and (b) against temperature (T) for the PVC/ASA (100/60 by weight) blend. [Color figure can be viewed in the online issue, which is available at wileyonlinelibrary.com.]

synergetic effect arising from component interactions. Figure 5(b) shows notched Charpy impact strength as a function of T for the PVC/ASA (100/60) blend. Impact strength at $T < 20°C$ is less than 10 kJ/m^2 while it is close to 60 kJ/m^2 at 60°C. Appearance observation demonstrated that the fractured samples exhibited light stress whitening in a small volume of the material near the notch tips at $T < 20°C$ and intensive stress whitening $T = 60°C$, which is related to the activated crazing happened at higher temperatures. The BDT is related to plastic deformation proceeded along with crack propagation at temperatures even far below the α-transition.[9]

Figure 6 shows SEM micrographs of PVC/ASA blends impact fractured at 30°C. Pure PVC exhibits a typical brittle failure

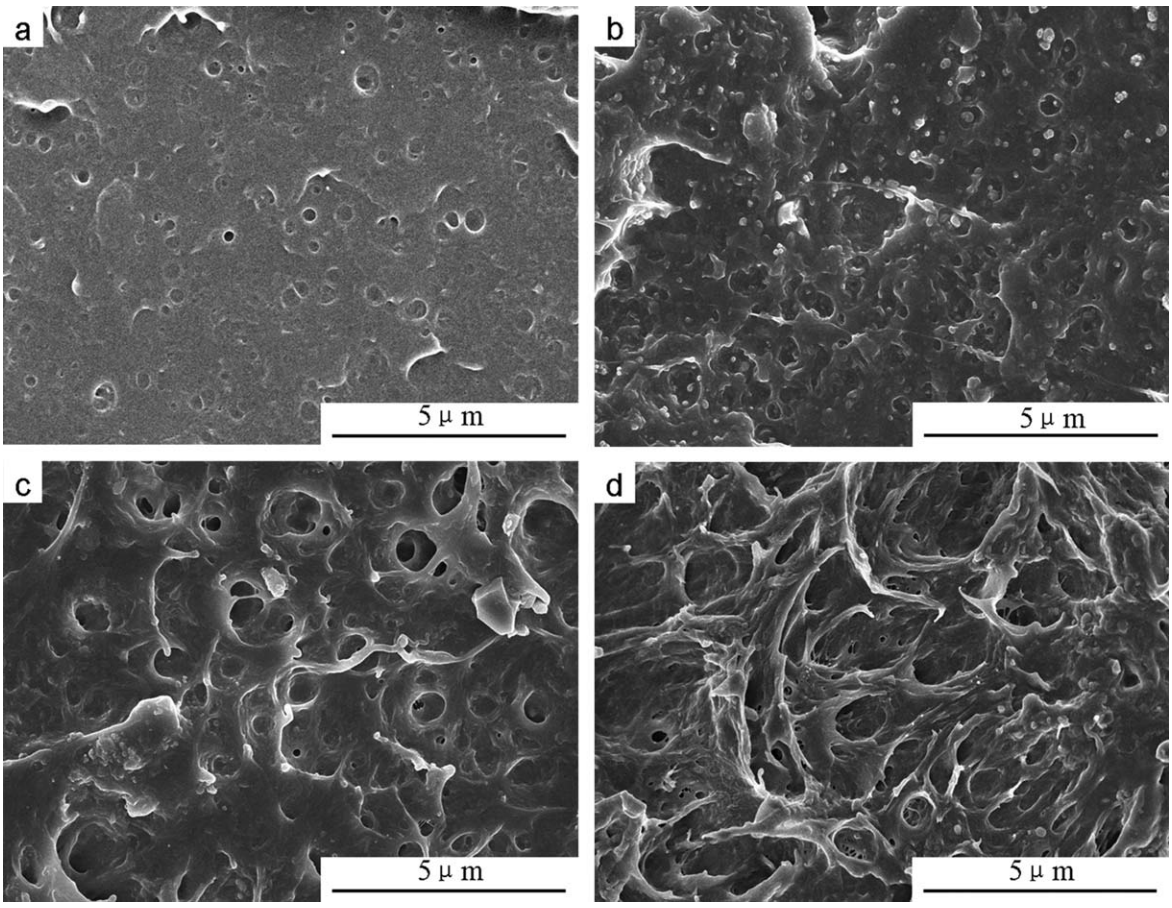

Figure 6. SEM morphologies of PVC/ASA blends containing (a) 0 phr, (b) 20 phr, (c) 60 phr, and (d) 100 phr ASA.

Applied Polymer SCIENCE

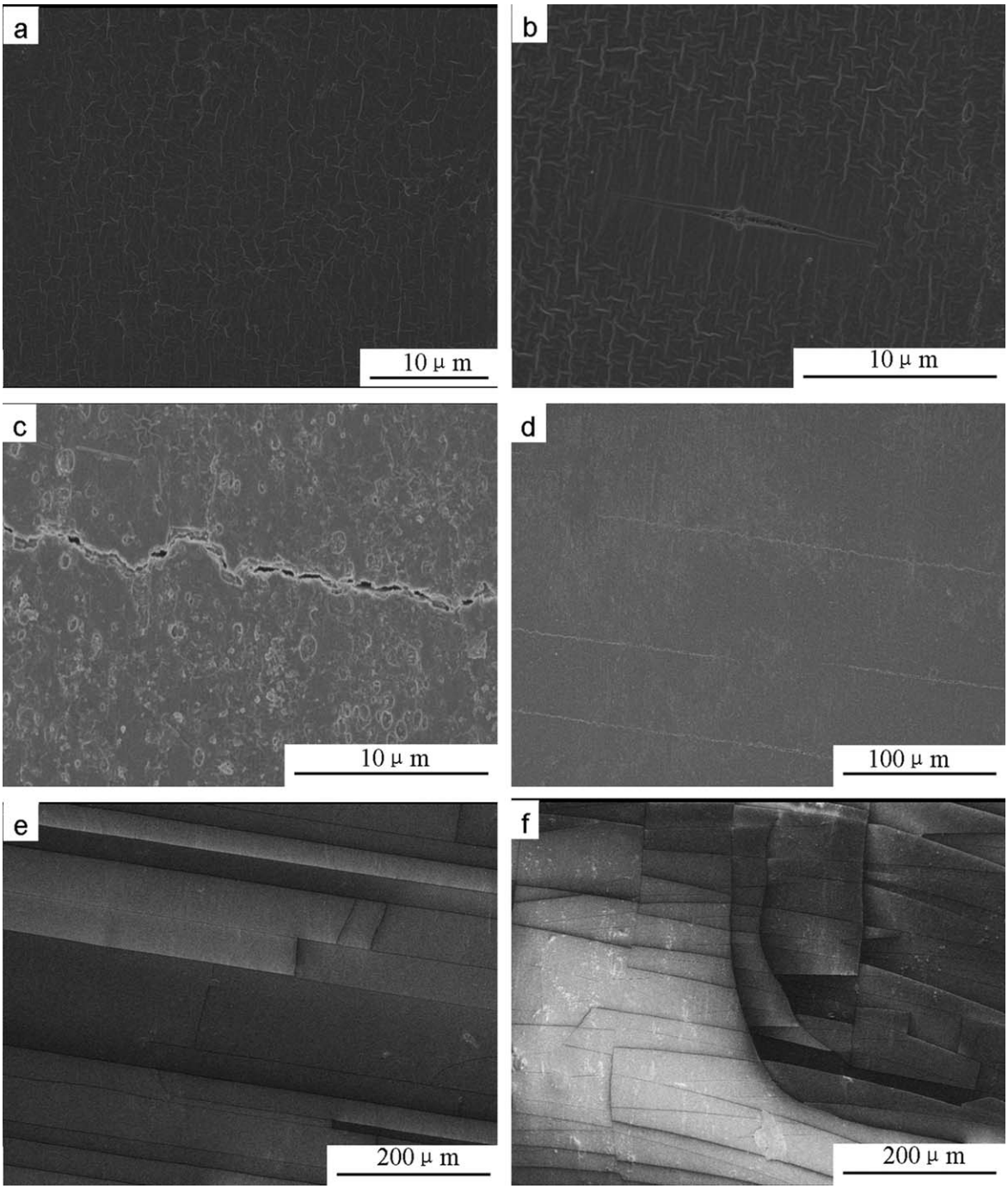

Figure 7. Appearance of PVC samples after UV irradiation of (a) 0, (b) 7, (c) 14, (d) 21, (e) 35, and (f) 42 days.

characteristic with smooth surface. The blend with 20 phr ASA shows some ductile characteristics with rather coarse laminated and corrugated fracture surface. At 60 phr ASA, the surface abounds with microvoids assigned to cavitation of the rubber phase under impact actions. At 100 phr ASA, the fracture surface exhibits highly sheared and dislocated microfibril morphology with abundant cavitation. It is clear that the rubbery particle in ASA rather homogenously dispersed in the PVC matrix is able to promote cavitation under rapid impact action, which causes changes in stress distribution of the matrix in the neighborhood of the cavitated particle and initiates massive shear yielding in the matrix.[9] Both cavitation and shear yielding could absorb massive impact energy so that ASA could effectively toughen PVC.

In Figure 5 for impact toughness, the optimum level of ASA incorporated the blend is dependent on temperature. The blend with 60 phr ASA is selected as an example for studying the influence of UV stability of PVC. Figures 7 and 8 show surface changes of PVC and PVC/ASA (100/60) blend samples

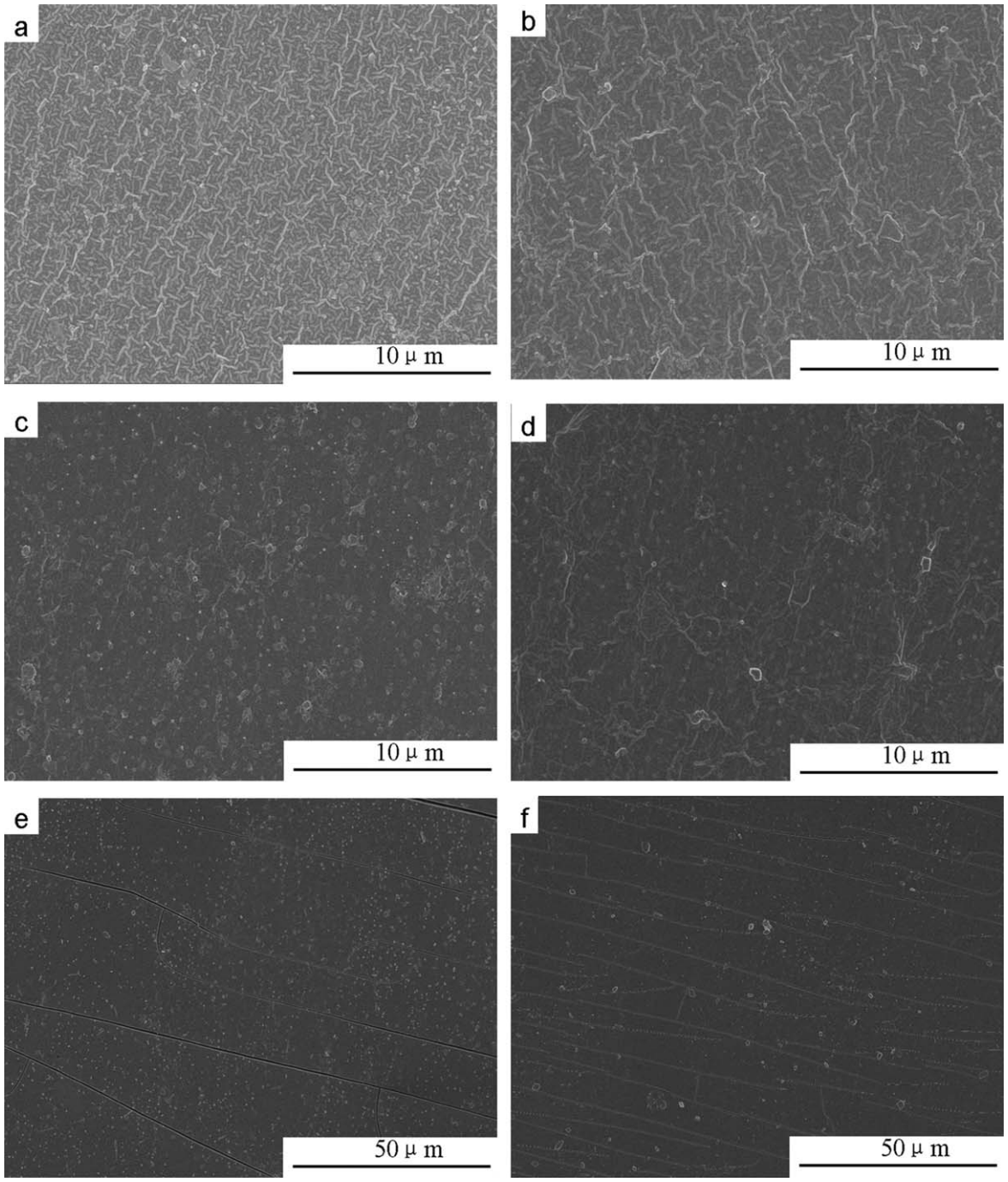

Figure 8. Appearance of PVC/ASA (100/60 by weight) samples after UV irradiation of (a) 0, (b) 7, (c) 14, (d) 21, (e) 35, and (f) 42 days.

after UV irradiation. There appear intensive flaws on the surface of PVC samples after 7 days of exposure and microcracks as large as 10 μm in length after 14 days of exposure (Figure 7). After UV irradiation of 35 days, the even surface of PVC has been completely destroyed with appearance of layered strips. These appearance variations under intensive UV irradiation are caused by serious chemical reactions such as dehydrochlorination, oxidation, and chain scission and crosslinking.[32] Compared with PVC samples, the surface of aged PVC/ASA blend has a great improvement (Figure 8). The blend exhibits smooth surface after 7 days of irradiation while few small chalked granules appear on the surface until 14 days. The layered strips appear after 35 days while the strip interval is considerably smaller than that of PVC. The PVC/ASA blend has an improve UV resistance due to consumption of energy by vibration and free rotation of ester bonds of ASA.[33] Furthermore, the interaction of the local dipoles between chlorines of PVC and the ester carbonyl groups in ASA may delay the detachment of the labile chlorine atoms from PVC under UV irradiation.[28]

Applied Polymer SCIENCE

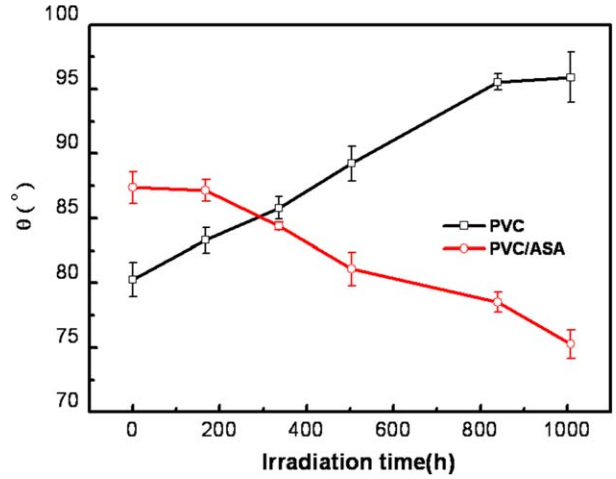

Figure 9. Contact angles (θ) of PVC and PVC/ASA (100/60 by weight) blend as a function of irradiation time. [Color figure can be viewed in the online issue, which is available at wileyonlinelibrary.com.]

Figure 9 shows the contact angle (θ) of PVC and PVC/ASA (100/60) blend after UV irradiation to different times. θ of PVC increases with increasing irradiation time while the reverse is true for the blend, which indicates that UV aging causes the formation of hydrophilic and hydrophobic surfaces on the PVC and the blend samples. The photo-oxidation of PVC includes photo-discoloration and photo-bleaching, related to the formation of polyenes from a non-oxidative photochemical reaction and photo-oxidation of these polyenes, respectively.[34] The latter is controlled by the oxygen diffusion. With the oxygen diffusion, the surface of PVC is activated by oxidation to form polar groups such as carbonyl, hydroxyl, and hydroperoxide groups during the UV irradiation.[35] Due to the protection of ASA that decelerates the oxygen diffusion, PVC in the blends mainly undergoes photo-discoloration reaction to give rise to hydrophobic surface with nonpolar groups.[34] The produced polyenes and polar groups in the photo-oxidated PVC macromolecules are tiny and are usually masked by the intrinsic absorbances of PVC and ASA in FTIR spectra.[36] The θ also indicates the roughness change of samples.[37] The surface of PVC (Figure 7) becomes rougher with increasing time of UV irradiation. However, the surface of the PVC/ASA (100/60) blend becomes much smoother after irradiation of 42 days (Figure 8).

Figure 10 shows DMA curves of PVC and PVC/ASA (100/60) blend before and after 30 days of UV irradiation. After the UV irradiation, T_β and T_g of PVC increase by 3 and 2°C, respectively, which is accompanied with improvement of E' in the whole temperature range investigated, implying the production of oxidation-crosslinking products[34] that restrict the molecular movement. The curve of aged PVC/ASA blend does not change obviously except for a small reduction in tan δ values, which indicates that the structure of PVC in blend changed slightly during the UV irradiation. Upon protection using ASA,[28] the functional groups such as cyano and ester groups can absorb the UV energy much easier than PVC and convert the energy into harmless heat by molecular auto-rotation and

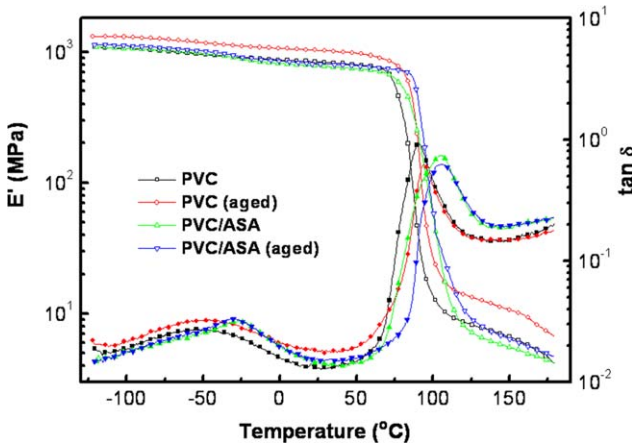

Figure 10. Storage modulus (E', hollow symbols) and loss factor (tan δ, solid symbols) against temperature (T) for PVC and PVC/ASA (100/60 by weight) blend before and after 30 days of UV irradiation. [Color figure can be viewed in the online issue, which is available at wileyonlinelibrary.com.]

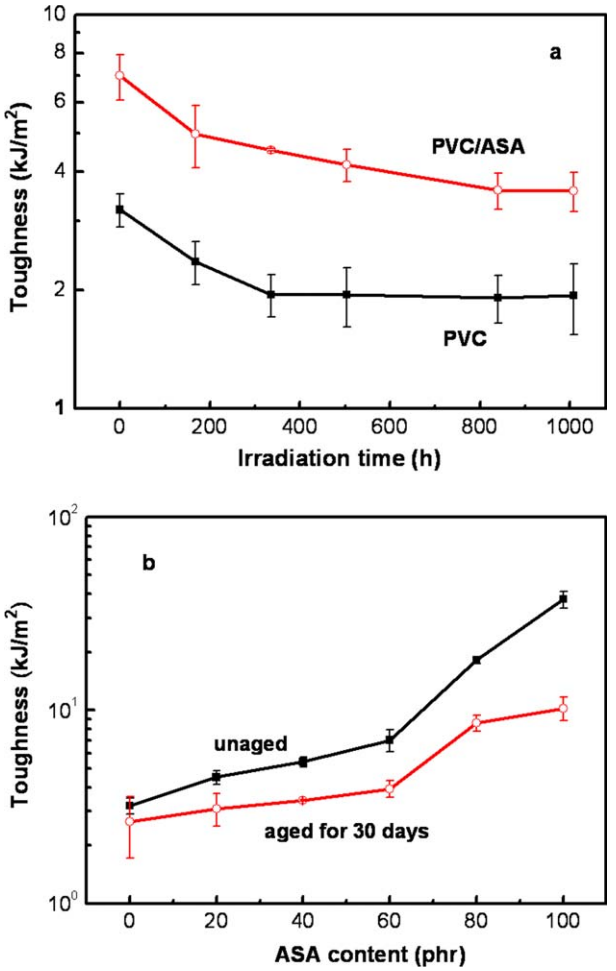

Figure 11. (a) Notched Charpy impact strength of PVC and PVC/ASA (100/60 by weight) blend as a function of irradiation time and (b) toughness variation of PVC/ASA blends before and after 30 days of UV irradiation. [Color figure can be viewed in the online issue, which is available at wileyonlinelibrary.com.]

recombination, which protects the blend from serious degradation and crosslinking.[32]

Figure 11(a) shows UV irradiation induced toughness changes for PVC and PVC/ASA (100/60) blend. Toughness of PVC and the blend decreases quickly with increasing irradiation time and levels off after 400 h while the aged blend exhibits roughness higher than PVC. The presence of ASA stress absorbers is one reason for the higher toughness of the aged blend while the synergetic effect between PVC and ASA might also play an important role. The improved UV resistance to the degradation of PVC contributes to improvement in toughness. Figure 11(b) shows irradiation induced toughness variations of the blends with different ASA contents. After 30 days of irradiation, toughness of blends containing 80 and 100 phr ASA is still larger than 10 kJ/m^2. These results indicate that the blends have good UV resistance and toughening effect to rigid PVC products. The PVC/ASA blends can be used for outdoor products with weatherability better than PVC.[13,38,39]

CONCLUSIONS

Toughness, heat resistance and thermal stabilization of the injection molded PVC/ASA blends were simultaneously improved with increasing ASA resin content. Based on the results from TEM and DMA, PVC had a good compatibility with ASA, which was responsible for the well dispersion of ASA in the matrix and the significant toughening effect related to cavitation and microfiber drawing. The blends exhibited a better UV irradiation resistance and demonstrated higher toughness after UV irradiation of 30 days in comparison with mold injected rigid PVC.

REFERENCES

1. Zhang, Z.; Chen, S.; Zhang, *J. Polym. Test.* **2011**, *30*, 534.
2. Zhang, Z.; Chen, S.; Zhang, J. *J. Vinyl. Addit. Technol.* **2011**, *17*, 85.
3. Liu, Z. H.; Zhang, X. D.; Zhu, X. G.; Li, R. K. Y.; Qi, Z. N.; Wang, F. S.; Choy, C. L. *Polymer* **1998**, *39*, 5019.
4. Zhang, L. X.; Zhou, C.; Sun, S. L.; Ren, L.; Ma, X. L.; Zhang, M. Y.; Zhang, H. X. *J. Appl. Polym. Sci.* **2010**, *116*, 3448.
5. Du, P. H.; Yu, J.; Lin, P. F.; Song Y. H.; Zheng Q. *Chinese J. Polym. Sci.* **2011**, *29*, 757.
6. Du, P. H.; Yu, J.; Lin, P. F.; Song Y. H.; Zheng Q. *Acta Polym. Sin.* **2011**, 1395.
7. Scott, G.; Tahan, M. *Eur. Polym. J.* **1977**, *13*, 989.
8. Belhaneche-Bensemra, N.; Bedda, A. *Macromol. Symp.* **2001**, *176*, 145.
9. Si, Q. B.; Zhou, C.; Yang, H. D.; Zhang, H. X. *Eur. Polym. J.* **2007**, *43*, 3060.
10. Ramteke, A. A.; Maiti, S. N. *J. Appl. Polym. Sci.* **2010**, *116*, 486.
11. Han, Y.; Tai, Z. X.; Zhou, C.; Zhang, M. Y.; Zhang, H. X.; Liu, F. Q. *Polym. Bull.* **2009**, *62*, 855.
12. Rimdusit, S.; Damrongsakkul, S.; Wongmanit, P.; Saramas, D.; Tiptipakorn, S. *J. Reinf. Plast. Comp.* **2011**, *30*, 1691.
13. DeArmitt, C. *Plastics, Add. Comp.* **2004**, *6*, 32.
14. Beltran, M.; Marcilla, A. *Eur. Polym. J.* **1997**, *33*, 1135.
15. Qian, Z.; Zhang, Z.; Song, L.; Liu, H. *J. Mater. Chem.* **2009**, *19*, 1297.
16. Aouachria, K.; Belhaneche-Bensemra, N. *Polym. Test.* **2006**, *25*, 1101.
17. McBrierty, V.; Douglass, D.; Kwei, T., *Macromolecules* **1978**, *11*, 1265.
18. l'Abee, R.; Li, W.; Goossens, H.; van Duin, M., *Macromol. Symp.* **2008**, *265*, 281.
19. Feng, H.; Shen, L.; Feng, Z. *Eur. Polym. J.* **1995**, *31*, 243.
20. Meier, R. J.; Struik, L. C. E. *Polymer* **1998**, *39*, 31.
21. Moon, H. S.; Choi, W. M.; Kim, M. H.; Park, O. O. *J. Appl. Polym. Sci.* **2007**, *104*, 95.
22. Kalouskova, R.; Novotna, M.; Vymazal, Z. *Polym. Degrad. Stab.* **2004**, *85*, 903.
23. Arkis, E.; Balkose, D. *Polym. Degrad. Stab.* **2005**, *88*, 46.
24. Liu, Y. B.; Liu, W. Q.; Hou, M. H. *Polym. Degrad. Stab.* **2007**, *92*, 1565.
25. Fang, L.; Song, Y.; Zhu, X.; Zheng, Q. *Polym. Degrad. Stab.* **2009**, *94*, 845.
26. Gonzalez-Ortiz, L. J.; Arellano, M.; Sanchez-Pena, M. J.; Mendizabal, E.; Jasso-Gastinel, C. F. *Polym. Degrad. Stab.* **2006**, *91*, 2715.
27. Shah, B. L.; Shertukde, V. V. *J. Appl. Polym. Sci.* **2003**, *90*, 3278.
28. Tawfik, S. Y.; Asaad, J. N.; Sabaa, M. W. *Polym. Degrad. Stab.* **2006**, *91*, 385.
29. Feldman, D.; Rusu, M. *Eur. Polym. J.* **1970**, *6*, 627.
30. Wang, Q. G.; Zhang, X. H.; Liu, S. Y.; Gui, H.; Lai, J. M.; Liu, Y. Q.; Gao, J. M.; Huang, F.; Song, Z. H.; Tan, B. H.; Qiao, J. L. *Polymer* **2005**, *46*, 10614.
31. Takemori, M. T. *Polym. Eng. Sci.* **1979**, *19*, 1104.
32. Ye, X.; Pi, H.; Guo, S. *J. Appl. Polym. Sci.* **2010**, *117*, 2899.
33. Pi, H.; Chen, S. Q.; Guo, S. Y. *Chem. J. Chinese U.* **2009**, *30*, 1029.
34. Gardette, J.; Gaumet, S.; Philippart, J. *J. Appl. Polym. Sci.* **1993**, *48*, 188.
35. Shi, W.; Zhang, J.; Shi, X. M.; Jiang, G. D. *J. Appl. Polym. Sci.* **2008**, *107*, 528.
36. Fang, L.; Song, Y. H.; Zhu, X. N.; Chen, S. H.; Du, P. H. *Chinese J. Polym. Sci.* **2010**, *28*, 637.
37. Mirji, S. *Surf. Interface Anal.* **2006**, *38*, 158.
38. O'neill, M. A. *US Patent* 4,910,067, **1990**.
39. Hills, R. A. *US Patent* 6,752,941, **2004**.